PHYSICAL REVIEW C VOLUME 48, NUMBER 5 NOVEMBER 1993

Core polarization phenomena in pion-nucleus charge-exchange reactions above the delta resonance

E. Oset
Departamento de Física Teórica and Instituto de Física Corpuscular, Centro Mixto Universidad de Valencia, CSIC, 46100 Burjassot, Valencia, Spain
and Institute for Nuclear Theory, University of Washington, Seatle, Washington 98195

D. Strottman
Theoretical Division, Los Alamos National Laboratory, Los Alamos, New Mexico 87545
and Institute for Nuclear Theory, University of Washington, Seatle, Washington 98195

H. Toki
Physics Department, Tokyo Metropolitan University, Tokyo 192, Japan
and Institute for Nuclear Theory, University of Washington, Seattle, Washington 98195

J. Navarro
Departamento de Física Atómica, Molecular y Nuclear and Instituto de Física Corpuscalar, Centro Mixto Universidad de Valencia, CSIC, 46100 Burjassot, Valencia, Spain
(Received 3 May 1993)

We study pion-induced single- and double-charge exchange reactions in nuclei at energies above the $\Delta(3/2,3/2)$ resonance using a microscopic, parameter-free Glauber approach. We introduce corrections in the amplitudes due to the medium polarization from an isospin-flip spin-nonflip source which dominates the reaction in the transitions studied and which has not previously been identified. Using an effective force derived from the study of electromagnetic transitions we obtained sizable reductions of the cross sections in both single- and double-charge exchanges, which bring the results of both reactions into close agreement with experiment. Predictions for angular distributions for both reactions on ^{14}C, ^{18}O, and ^{42}Ca targets are made which should serve as guidelines for experiments planned in this region and as further tests of the proposed isovector renormalization.

PACS number(s): 25.80.Gn, 24.30.Gd

I. INTRODUCTION

The study of pion-nucleus reactions above the region of the delta resonance has begun with experiments of elastic and inelastic scattering [1], single-charge-exchange (SCX) [2]and double-charge-exchange reactions (DCX). [3] Simultaneously, theoretical work on these higher energies has been initiated on elastic or inelastic scattering [4–8], single-charge exchange [2,9,10], and double-charge exchange [7,11,12]. For elastic scattering the agreement among the theoretical approaches and with experiment is fairly good. The discrepancies are at the level of 10%. For the charge-exchange reactions the agreement is less good. For SCX reactions the results of Refs. [2,10] overestimate the experiment while that of Ref. [9] is closer to experiment. For DCX reactions the work of Ref. [12] (without the isovector correction) overestimates the experimental cross section while that of Ref. [7] underestimates it. Additional work on the charge-exchange reactions along the lines of Refs. [7,9] is now in progress [13]. The work of Refs. [10,12] employed a Glauber model that used experimental πN experimental phase shifts and in which there were no free parameters; thus, the discrepancy with data seen at these higher energies is particularly troubling.

One of the motivations behind the study of these reactions at higher energies is the belief that the reaction mechanisms are simpler at higher energies than at resonance or at low energies. If this is the case, one should be able to look in a cleaner way at other aspects of the problem, such as nuclear structure details, polarization phenomena, etc. In support of the idea of a simpler reaction mechanism at higher incident pion energies is the fact that elastic scattering is fairly well reproduced at these energies with both a Glauber approach [4,5] and an optical potential approach [7] and that the pion absorption mechanisms in both SCX and DCX reactions [10,12] play a minor role.

From studies of the electromagnetic transitions in nuclei, it is known that the operators that describe such processes in nuclei are modified from their free space values. In the present paper we investigate how a nucleus is polarized when a pion source excites the nucleus and induces an isospin transition. We further investigate how the SCX and DCX cross sections are modified when this polarization is taken into account. One of the findings of the paper is that the consideration of this new phenomena is very important in charge-exchange reactions and one finds a fair agreement with experiment when the polarization is taken into account.

II. GLAUBER FORMALISM FOR SCX AND DCX REACTIONS

The Glauber formula for pion-nucleus reactions is given by

$$F_{M_i M_f}(q)=\frac{ik}{2\pi}\int d^2b\, e^{i\mathbf{q}\cdot\mathbf{b}}\left\langle J_f T_f M_f \left| 1-\prod_{j=1}^{A}(1-\Gamma_j)\right| J_i T_i M_i\right\rangle , \tag{1}$$

where $\mathbf{b}$ is the impact parameter, $\mathbf{k}$ the incident pion momentum, $\mathbf{q}=\mathbf{k}-\mathbf{k}'$ is the momentum transfer, and Γ_j is the profile function defined as

$$\Gamma_j(\mathbf{b}-\mathbf{s}_j)=\frac{1}{2\pi ik}\int d^2q\, e^{-i\mathbf{q}\cdot(\mathbf{b}-\mathbf{s}_j)}h(\mathbf{q}) \tag{2}$$

with $\mathbf{s}_j$ the projection of $\mathbf{r}_j$ onto the impact parameter plane. The momentum variables in Eq. (1) are laboratory variables while those in Eq. (2) are in the πN center-of-mass frame. The quantity $h(\mathbf{q})$ is the πN elementary amplitude

$$h(\mathbf{q})=f^{(s)}(\mathbf{q})+\boldsymbol{\Theta}\cdot\boldsymbol{\tau}f^{(v)}(\mathbf{q}) +i[g^{(s)}(\mathbf{q})+\boldsymbol{\Theta}\cdot\boldsymbol{\tau}g^{(v)}(\mathbf{q})]\boldsymbol{\sigma}\cdot\hat{\mathbf{n}} , \tag{3}$$

which contains an isoscalar (s) and isovector part (v) and a spin-independent and a spin-flip part. The operators $\boldsymbol{\Theta}$ and $\boldsymbol{\tau}$ are the isospin operators for the pion and the nucleon, respectively, and $\hat{n}=(\mathbf{k}\times\mathbf{k}')/|\mathbf{k}\times\mathbf{k}'|$. Details on the construction of the elementary amplitude from experimental phase shifts, and questions concerning time ordering in the Glauber formula and other technical details are discussed in Ref. [10]. The plane shifts and inelasticity parameters are those of 1987 analysis of Arndt [14]. The πN amplitudes were calculated including partial waves up to an l of 5. Effects of spin flip are included.

The formulas which arise for the SCX and DCX amplitude for (π^+,π^0) and (π^+,π^-) reactions are

$$F^{\mathrm{SCX}}(\mathbf{q})=\frac{ik}{2\pi}\int d^2b\, e^{i\mathbf{q}\cdot\mathbf{b}}\langle\psi_f|\sum_j\sqrt{2}\Gamma_j^{(v)}\tau_j^+\prod_{l\neq j}(1-\Gamma_l^{(s)})|\psi_i\rangle , \tag{4}$$

$$F^{\mathrm{DCX}}(\mathbf{q})=\frac{ik}{2\pi}\int d^2b\, e^{i\mathbf{q}\cdot\mathbf{b}}\langle\psi_f|-2\sum_{i<j}\Gamma_i^{(v)}\Gamma_j^{(v)}\tau_i^+\tau_j^+\prod_{l\neq i,j}(1-\Gamma_l^{(s)})|\psi_i\rangle , \tag{5}$$

where $\Gamma^{(s)}$ and $\Gamma^{(v)}$ are obtained from Eq. (2) by replacing $h(\mathbf{q})$ by the corresponding isoscalar and isovector pieces of Eq. (3). The factors $\Gamma^{(v)}\tau^+$ induce the charge-exchange transition while the factor $\prod(1-\Gamma^{(s)})$ accounts for the distortion of the pion waves.

Since the operator in Eqs. (4) and (5) is a sum of the product of A one-body operators, if the shell-model wave functions are determinants, then the evaluation of Eqs. (4) and (5) reduces to the evaluation of a sum of $A\times A$ determinants. By using the Glasgow shell-model code [15], the wave functions are naturally expressed as a sum of Slater determinants, and hence, antisymmetry is explicitly included. The nuclear wave functions for ^{18}O and ^{18}Ne were obtained using matrix elements obtained by Kuo [16]. The wave functions for mass 14 were obtained using the matrix elements of Cohen and Kurath [17]. Oscillator parameters obtained from electron scattering of $\alpha^2=0.39$ fm^{-2} for ^{14}C and 0.319 fm^{-2} for ^{18}O were used. Thus, this calculation has no free parameters.

In this paper we study transitions to the isobaric analog state in SCX reactions and to the double isobaric analog state in DCX reactions, as well as transitions to selected excited levels. A single-step charge-exchange transition is depicted diagrammatically in Fig. 1(a). However, in the case of closed-shell nuclei plus additional particles in the valence shell, only the latter particles participate *directly* in the charge-exchange process because of Pauli blocking in the core. In the case when one has multiple elastic steps in addition to charge exchange, as is the case in strongly interacting particles, the core particles can also participate in the charge-exchange process if fully antisymmetric A-body wave functions are used. These effects are important around the Δ resonance [18] since there are many multiple scattering steps, but are less relevant at energies above the Δ resonance where the pion-nucleon cross section is appreciably reduced and the pion mean free path is larger.

There is, however, another way to allow the core particles to participate in the charge-exchange reaction. This is through the polarization of the medium by the pion source. This is depicted diagrammatically in Figs. 1(b), 1(c), and 1(d). The pion scatters from particle-hole components different than the final one. These particle-hole components then propagate through the nucleus by means of the residual nuclear interactions and finally couple to the desired final state in our chosen space of wave functions. We shall include these effects through the methods discussed in the next section.

III. MEDIUM POLARIZATION IN THE CHARGE-EXCHANGE TRANSITIONS

The nucleon-nucleon residual interaction is conveniently parametrized in the Landau-Migdal form [19]

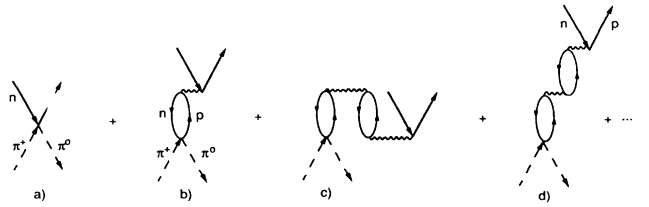

FIG. 1. Diagrammatic expression of the medium polarization in the isospin channel through ph excitation iterated in a random phase approximation form.

as

$$V(\mathbf{r}_1,\mathbf{r}_2)=(f_0+f_0'\tau_1\cdot\tau_2+g_0\sigma_1\cdot\sigma_2 +g_0'\sigma_1\cdot\sigma_2\tau_1\cdot\tau_2)\delta(\mathbf{r}_1\cdot\mathbf{r}_2)\ ; \quad (6)$$

the values of the parameters have been deduced from a systematic study of electromagnetic transitions in electron scattering and described in the work of Speth, Werner, and Wild of Ref. [20].

The spin-flip terms in the πN interaction play a negligible role unless specific transitions that are sensitive to these components are chosen. In our study of transitions to isobaric analog states in this paper they are not important. As a consequence, the g_0' term of the effective interaction, Eq. (6), plays little role in the polarization. The term $f_0'\tau_1\cdot\tau_2$ is primarily responsible for the propagation of the neutron hole-proton particle excitation induced by the charge-exchange steps in Fig. 1.

In an infinite nuclear medium of constant density ρ, this polarization of the medium leads to an isovector renormalization of the charge-exchange amplitude. This isovector renormalization is given by

$$f^{(v)}(q)\rightarrow\frac{f^{(v)}(q)}{1-f_0'U(q^0=0,q,\rho)}\ , \quad (7)$$

where $U(q^0,q,\rho)$ is the Lindhard function for a particle-hole (ph) excitation of Ref. [21]. An extra factor of 2 must be included with respect to Ref. [21] to account for the isospin factor coming from the $\tau_1\cdot\tau_2$ operator. The Lindhard function in Eq. (7) is defined as

$$U(q^0,q,\rho)=4\int\frac{d^3k}{(2\pi)^3}\left[\frac{n(\mathbf{k})[1-n(\mathbf{k}+\mathbf{q})]}{q^0+\epsilon(\mathbf{k})-\epsilon(\mathbf{k}+\mathbf{q})+i\epsilon}+\frac{n(\mathbf{k})[1-n(\mathbf{k}-\mathbf{q})]}{-q^0+\epsilon(\mathbf{k})-\epsilon(\mathbf{k}-\mathbf{q})+i\epsilon}\right], \quad (8)$$

where $\epsilon(\mathbf{k})$ is the kinetic energy of the nucleon and $n(\mathbf{k})$ stands for the occupation number of the Fermi sea.

One may get a rough idea of the isovector renormalization effects in finite nuclei by choosing the density most likely probed in the process and substituting it into the Lindhard function in Eq. (8). However, while this would be fair for processes in which values of q^0 are large compared to the ordinary nuclear excitation energies, in the present case there is either no transfer of energy, ($q^0=0$), or the transfer is very small, and one must be more cautious. Indeed, the function $U(q^0=0,q,\rho)$ has a finite limit as $q\rightarrow 0$. (Note that in Eq. (8) one gets an indeterminate result of the type 0/0 in this case, but which has a finite limit when the formula of Ref. [21] is evaluated.) In a finite closed-shell nucleus there is no transition with $\mathbf{q}=0$ allowed from the core to excited states. This is because the matrix element

$$\frac{\langle\phi_n|e^{i\mathbf{q}\cdot\mathbf{r}}|\phi_0\rangle}{\epsilon_{\rm ph}} \quad (9)$$

involved in the calculation of the ph excitation is zero. The reason for the vanishing of Eq. (9) is that the numerator vanishes while the particle-hole excitation energy $\epsilon_{\rm ph}$ has a minimum value different than zero. This is a source of difference between the infinite medium case—where this minimum excitation energy is zero as one can see in Eq. (8)—and the finite nucleus case.

A more realistic evaluation of the Lindhard function in the limit of $q^0=0$ must take into account this minimum excitation energy Δ; this will automatically bring $U(q^0=0,q)$ to zero in the limit $\mathbf{q}\rightarrow 0$. We have done this and the results appear in the Appendix.

In Fig. 2 we plot the Lindhard function at $q^0=0$ with gaps of 5 and 3 MeV for two different densities. The two upper curves correspond to $\rho=\frac{1}{2}\rho_0$ (ρ_0 being normal nuclear matter density) with a gap of $\Delta=5$ and 3 MeV, respectively. The next two lower curves correspond to the same values of Δ but for $\rho=\rho_0$. Finally, the lowest curve is the ordinary Lindhard function at $q^0=0$ and $\rho=\rho_0$, or equivalently the new Lindhard function for $\Delta=0$. As we can see, the main effect of the gap is to force the Lindhard function to go to zero as $q\rightarrow 0$. As a consequence of this, the differences between the new Lindhard function and the ordinary one, for small values of q, are quite large. At large values of q the two Lindhard functions coincide independent of the value of the gap. We also observe that the differences between the Lindhard function with $\Delta=3$ or 5 MeV are small and hence the uncertainties induced in the results by our approximation should also be small once we choose a reasonable value for the gap corresponding to a realistic case. We have chosen $\Delta=5$ MeV for our calculations.

The parameter f_0' in the Landau-Migdal parametrization of the nucleon-nucleon interaction, Eq. (6), is taken from Ref. [20]. A smooth density dependence, also tak-

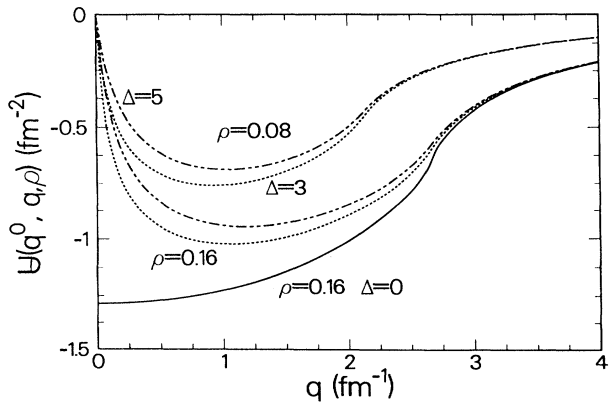

FIG. 2. Modified Lindhard function $U(q^0,q,\Delta,\delta)$, with a gap Δ for a minimum ph excitation energy, calculated at $q^0=0$ for different densities and different values of Δ. The two upper curves for $\rho=\rho_0/2(0.08\ \text{fm}^{-3})$ and two values of the gap $\Delta=5$ and 3 MeV. The two middle curves correspond to the same values of the gap but $\rho=\rho_0$ (0.17 fm^{-3}). The lower curve corresponds to ρ_0 with no gap which is the ordinary Lindhard function [21].

en from Ref. [20], is assumed for this parameter:

$$f_0'(\rho)=c_0\left[\left[\frac{\rho(r)}{\rho(0)}\right]f_0'^{(\mathrm{in})}+\left[1-\frac{\rho(r)}{\rho(0)}\right]f_0'^{(\mathrm{ex})}\right], \quad (10)$$

where $f_0'^{(\mathrm{in})}=0.33$ and $f_0'^{(\mathrm{ex})}=0.45$ describe the internal and external regions of the nucleus, and $c_0=380$ MeV fm^3. We have used a three-parameter Fermi distribution for the form of the density distribution $\rho(r)$; the parameters were taken from de Vries, de Jager, and de Vries [22].

Assuming a local density $\rho=\rho(r)$, Eq. (7) produces a renormalization of the isovector amplitude depending on both q and $\rho(r)$. This renormalization is particularly easy to implement in the framework of Glauber theory since the profile function is constructed from an integral involving both spatial and momentum coordinates. Hence, the isovector renormalization due to polarization is implemented here with the change

$$\Gamma_j^{(v)}(\mathbf{b}-\mathbf{s}_j)\rightarrow\Gamma_j^{(v)}(\mathbf{b}-\mathbf{s}_j,r_j)=\frac{1}{2\pi ik}\int d^2q\, e^{-i\mathbf{q}\cdot(\mathbf{b}-\mathbf{s}_j)}f^{(v)}(\mathbf{q})\frac{1}{1-f_0'(\rho(r_j))U(q^0=0,q,\Delta,\rho(r_j))}\,. \quad (11)$$

This integral must be performed numerically.

In the absence of multiple scattering the Glauber approach reproduces the impulse approximation. In this case, if we look at SCX in the forward direction, $q=0$, and there is no renormalization since $U(q^0=0,q=0,\Delta,\rho)$ will be zero. Hence any renormalization appearing in SCX at forward angles must be a consequence of multiple scattering in which the charge-exchange reaction results in a pion momentum of finite angle and some previous or posterior elastic collision brings the total scattering angle back to zero.

In contrast a double-charge exchange can result in a scattering at zero degrees as it can arise from situations where there have been two charge exchange steps with finite and opposite angles (this is assuming no additional elastic steps). With extra elastic steps there can be further contributions from larger scattering angles, or equivalently larger values of q. As a consequence, one might expect at forward angles in DCX a renormalization factor larger than the square of the renormalization factor in SCX at the same angles.

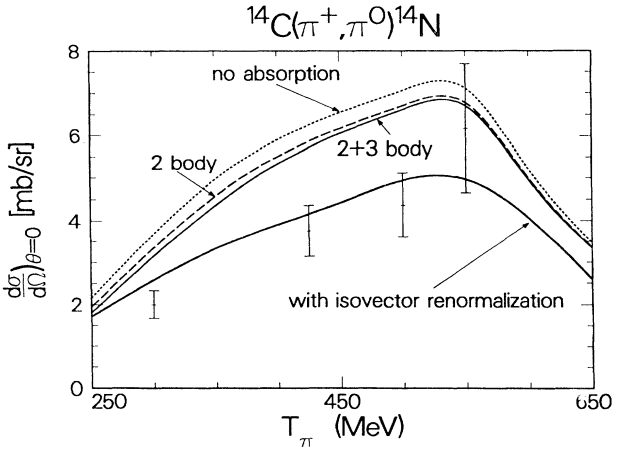

FIG. 3. Calculated differential cross section at zero degrees in the laboratory system for a SCX reaction on ^{14}C to the IAS in ^{14}N. The upper curves correspond to the results without polarization with or without inclusion of pion absorption [5]. The lower curve corresponds to the results obtained including absorption and the effects of isovector polarization. The experimental data are from Ref. [2].

IV. RESULTS AND DISCUSSION

We have performed calculations both for SCX and DCX reactions on two nuclei, ^{14}C and ^{18}O where there are some experimental data. We compare with the experimental results and make predictions for angular distributions which are not yet measured.

In Fig. 3 we show the results for a SCX reaction to the isobaric analog state (IAS) in ^{14}C at zero angle and compare the results with the experimental ones of Ref. [2]. In the absence of the medium isovector renormalization the theoretical results overestimate the experiment by about 30–35%. This was already noticed in Ref. [10] where it was shown that inclusion of pion absorption made only minor modifications at the level of 10%. When the isovector polarization effects are included we find an appreciable decrease of the cross sections of about 25–30%, which brings our results into close agreement with the experimental data.

In Table I we show similar results for DCX to the double isobaric analog state in ^{14}C and ^{18}O. The results are at 5° where the experiments were done [3]. The discrepancies between the theoretical results without polarization and the experiment are about a factor of 3–4 and are rather independent of the energy in the energy range of the table. When the isovector polarization is included there is a sizeable decrease of the cross section which brings the results into close agreement with the experimental data. As we discussed in Sec. III, with zero-momentum transfer there is no renormalization of the

TABLE I. The center-of-mass differential cross section in μb/sr at 5° for the (π^+,π^-) reaction leading to the ground state of the resultant nucleus. The experimental results are from Williams *et al.* [3]. The column TH are the results without polarization and the column headed THP are the results including the effects of the isovector medium polarization.

	^{14}C			^{18}O		
T_π (MeV)	Experiment	TH	THP	Experiment	TH	THP
300	3.84±0.54	11.9	3.0	2.68±0.37	8.9	3.0
350	4.15±0.42	14.8	3.6	3.00±0.27	9.4	3.0
400	3.24±0.39	15.1	3.8	3.06±0.29	8.9	2.8
450		14.2	3.7	2.94±0.33	8.1	2.6
500	3.62±0.65	13.7	3.8	2.69±0.35	7.7	2.6
525		13.5	3.7	2.65±0.80	7.5	2.6

elementary amplitude. Hence, the distortion, or multiple scattering, must be responsible for the renormalization of the SCX at zero degrees. In the case of DCX one could have two sequential charge-exchange processes with opposite angles contributing to the forward cross section. This would introduce renormalization effects even in the absence of distortion. We would hence anticipate the renormalization factor in DCX to be larger than the square of the factor found in SCX, and this is indeed the case as an inspection of Fig. 3 and Table I shows.

According to the same arguments, if we look at the angular distribution in SCX reactions the renormalization effects should be larger at finite angles, at least up to around $q=1$ fm^{-1}, where according to Fig. 2 the Lindhard function has its maximum absolute value. At $T_\pi=500$ MeV this means angles around 10°. In Fig. 4 we plot the differential cross section for SCX on ^{14}C at $T_\pi=500$ MeV, both with and without the isovector renormalization and compare the results with the data of Ref. [2]. There are only three pieces of data up to 6°. The agreement of our results with these data is fine. On the other hand, as we have anticipated, the results with the isovector renormalization have a stronger falloff as a function of the angle than do the unrenormalized results. Indeed, at zero degrees the isovector renormalization reduces the cross section by about 30% while from 10° to 15° the effect of the renormalization is a decrease of the cross section by a factor of 2.5–3. More data at larger angles would be welcome as a further test of the isovector renormalization.

In Fig. 5 we show the differential cross section for a SCX reaction on ^{14}C at $T_\pi=400$ MeV for the excitation of the IAS and two excited states. The excitation of the IAS dominates the cross section at small angles, while the 2^+ dominates at angles around 30°. The 1^+ gives only a small contribution.

In Fig. 6 we show the results for the differential cross section for the DCX reaction ^{18}O$(\pi^+,\pi^-)^{18}$Ne for the ex-

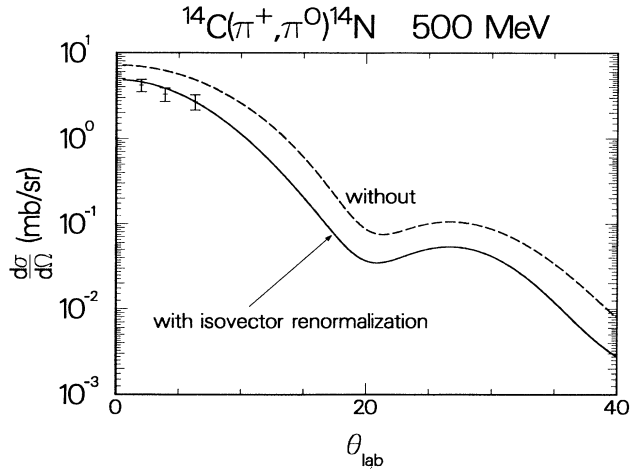

FIG. 4. Differential cross section at $T_\pi=500$ MeV for SCX on ^{14}C to the IAS as a function of the angle in laboratory variables. The upper curve shows the results obtained without isovector renormalization while the lower curve includes the polarization correction. The data are from Ref. [2].

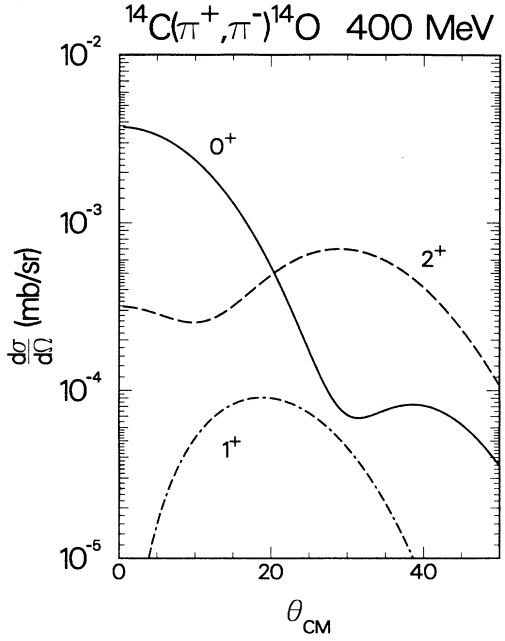

FIG. 5. Differential cross section at $T_\pi=400$ MeV for SCX on ^{14}C to the IAS and two excited states as a function of the c.m. angle.

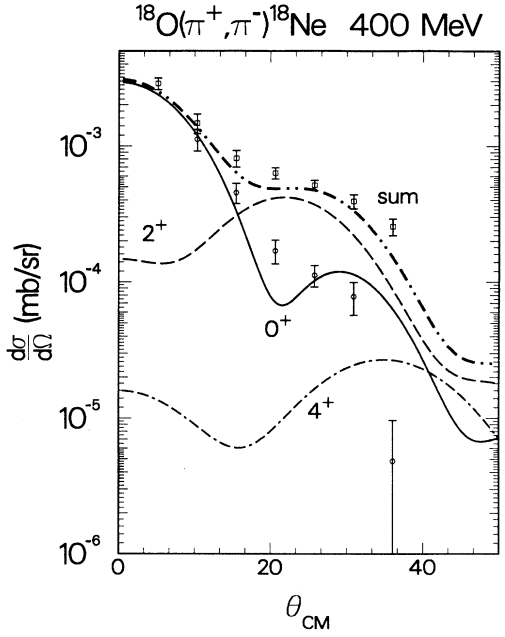

FIG. 6. Differential cross section for DCX on ^{18}O to the double isobaric analog state and two excited states in ^{14}N as a function of the c.m. angle. The sum of the 0^+ and 2^+ excitation is also shown in order to compare with the data of Ref. [3]. Squares: results of Ref. [3] for the sum of the cross section. Circles: excitation of the cross section to the double isobaric analog state [3] (see text).

citation of the double isobaric analog state, the ground state of ^{18}Ne, and for the excitation of the first excited state, the 2^+ state at 1.89 MeV. Results for the excitation of the 4^+ state at 3.56 MeV are also shown. For the double isobaric analog state, which provides the dominant contribution, we have used accurate $1d_{5/2}2s_{1/2}$ wave functions, while only $1d_{5/2}$ wave functions are used for the excited states. The inclusion of the $1d_{5/2}2s_{1/2}$ components increases the cross section for the double isobaric analog state by about 20% here, a moderate amount compared with the effects found at resonance where an increase of about a factor of 2 in the cross section was found [18]. We compare our results with those of Ref. [3]. In this latter work the combined contribution of the ground state and the 2^+ state was given since the energy resolution was not sufficient to separate the states [23].

As we can see from the theoretical results, the two states give rise to very different structures. The double isobaric analog state excitation gives rise to a pattern typical of elastic scattering with a diffraction minimum around 20° and a second maximum around 26°. The excitation of the 2^+ state gives rise to a different pattern which comes primarily from the addition of the $\Delta M=0$ and ± 2 contributions (M is the third component of the total angular momentum). The $\Delta M=\pm 1$ contribution which must arise through spin-flip processes is very small. The cross section is flat at small angles where the $\Delta M=0$ transition dominates and rises at higher angles where the $\Delta M=\pm 2$ transition takes over. While at small angles the strength for the excitation of the double isobaric analog state is about 20 times bigger than the corresponding one for the 2^+ state, at 22° where the excitation of the 2^+ state has a maximum, the strength of this latter state is about 6 times bigger than the corresponding one for the double isobaric analog state (DIAS). In fact, the peak of the 2^+ state is approximately at the same angle at which the double isobaric analog state distribution has a minimum.

The results for the sum of the two cross sections compare fairly well with those of Ref. [3]. In Ref. [3] the authors also made an analysis in order to extract the angular distribution for the excitation of the double isobaric analog state by assuming the total angular distribution to be made up of two peaks and performing a best fit to the data. The values extracted for the double isobaric analog state distribution are in qualitative agreement with our results. Obviously, with the assumption in Ref. [3] of two states, each with a diffraction structure allowing only one maximum, one necessarily misses the structure which we found for the double isobaric analog state and the excited 2^+. One has in this latter case three peaks. The clean separation of these states with an improved resolution in the experiments would be most desirable for a better comparison with the theoretical results. Some thoughts along this direction are presently underway [23].

Finally, in Fig. 7 we show the results for $d\sigma/d\Omega$ for DCX in ^{42}Ca. We show again the results for the excitation of the DIAS and the first excited state. The features are very similar to those found in ^{14}C or ^{18}O, only the minimum of the distribution for the ground state moves to smaller angles, as a consequence of the increased nuclear size. The effect of the polarization is similar to the one found for the lighter nuclei.

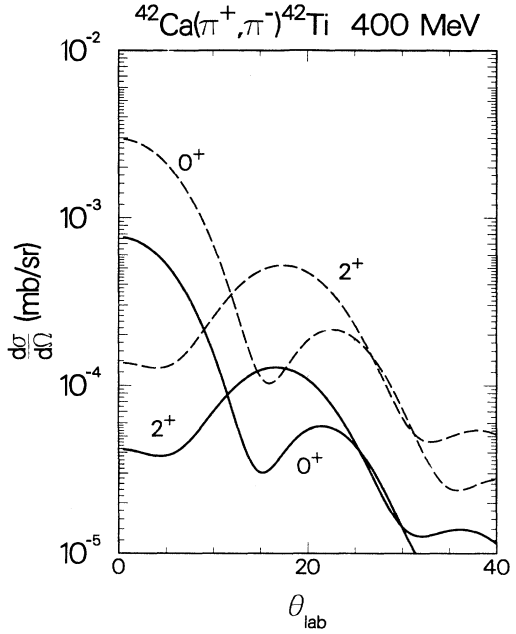

FIG. 7. Differential cross sections for DCX on ^{42}Ca to the ground state and first excited state of ^{42}Ti. The upper curves for each angular momentum correspond to the results obtained without polarization and the lower ones to the corresponding ones obtained including polarization. Partial waves through $l=5$ were included in the calculation.

As we indicated, we have considered pion-nucleon partial waves up to $l=5$ where good convergence was found. If one retains only s and p waves one gets a cross section for ^{42}Ca smaller by about a factor 2.3 than the cross section retaining all the necessary partial waves. As we can see in the figure the effect of the polarization is a decrease of the cross section by about a factor of 4, similar to what was also found for the cases of ^{14}C and ^{18}O.

V. CONCLUSIONS

We have studied SCX and DCX reactions at energies above the (3,3) resonance where the Glauber approach becomes increasingly reliable. While the elastic scattering was fairly well reproduced in this approach, the charge-exchange processes were overestimated by about 30% in SCX and by more than a factor of three in DCX. The new feature introduced in this paper is that the isovector-spin nonflip amplitude, the leading piece in our approach for the transitions studied, is appreciably renormalized inside the nuclear medium. The pion acts as an external source of excitation which polarizes the isospin distribution in the nucleus and this reverts into an effective renormalization of the isospin-flip amplitude. For the effective nuclear interaction in the relevant isospin channel we took the same one that results from the analysis of electron-induced transitions in nuclei. Our

calculation hence does not have any free parameters. However, it should be noted that the penetration of the pion into the nucleus changes as a function of energy. Thus, the interaction may be a function of energy. Further, the density dependence may be quite different for an electron and our choice, although producing excellent agreement for $A=14$ and 18 may not be appropriate for heavier nuclei such as ^{42}Ca. Experiments for heavier nuclei are greatly desired.

The resulting medium isovector renormalization resulted in appreciable decreases of both the SCX and DCX calculated cross sections which are then compatible with experiment for the nuclei studied. The angular distributions are poorly known experimentally, either because there are few data as in SCX, or because the separation of the double isobaric analog state and the excited states contributions is only done in an approximate way as in DCX. The agreement so far is good within the approximations done to extract the experimental numbers; more precise data on angular distributions in different nuclei are needed. From the physical point of view our findings seem to indicate that, as the energy of the pion increases, the complicated many-body reaction mechanisms that one had at low energies and around resonance fade away and the pions come to see more the individual nucleons. As a consequence nuclear structure details such as the polarizability of the nuclei in different channels can show up more clearly as already observed in the electron scattering experiments. The richness of the pion-nucleon interaction with respect to the electromagnetic interaction allows the direct exploration of many nuclear properties unreachable or only indirectly reachable with electromagnetic probes, pointing at the pion-nucleon reactions at those energies as a rich and complementary source of information of nuclear structure details.

The results given in this paper provide a strong indication for a renormalization of the isovector non-spin-flip operator. However, additional and more accurate data will be required to provide an accurate estimate of the magnitude of this renormalization. We hope such data will be forthcoming from both LAMPF and particularly KEK experiments.

ACKNOWLEDGMENTS

We wish to thank George Burleson for helpful conversations and for providing the experimental data used in Fig. 6. H.T. thanks the University of Valencia where part of this work was done for their hospitality.

APPENDIX: THE LINDHARD FUNCTION WITH A GAP IN THE PARTICLE-HOLE EXCITATION ENERGY

We define

$$U(q^0,q,\Delta,\rho)=4\int\frac{d^3k}{(2\pi)^3}\left[\frac{n(\mathbf{k})[1-n(\mathbf{k}+\mathbf{q})]}{q^0+\epsilon(k)-\epsilon(\mathbf{k}+\mathbf{q})-\Delta+i\epsilon}+\frac{n(\mathbf{k})[1-n(\mathbf{k}-\mathbf{q})]}{-q^0+\epsilon(k)-\epsilon(\mathbf{k}-\mathbf{q})-\Delta+i\epsilon}\right]. \tag{A1}$$

The modifications to the ordinary Lindhard function come from substituting $q^0\rightarrow$[second term in Eq. (A1)]. However, one cannot simply make this replacement in the two terms of the ordinary Lindhard function because there are terms which cancel there and do not cancel now with those substitutions. We have performed a direct evaluation and find for $x\leq 2$;

$$\begin{aligned}\mathrm{Re}U(q^0,q,\Delta,\rho)=-\frac{2Mk_F}{\pi^2}\frac{1}{2x}\Bigg\{&x+\frac{1}{2}\delta+\frac{1}{2}(\nu-\delta)\ln\left|\frac{\nu-\delta+x^2-2x}{\nu-\delta}\right|-\frac{1}{2}(\nu+\delta)\ln\left|\frac{\nu+\delta-x^2+2x}{\nu+\delta}\right|\\&+\frac{1}{2}\left[1-\frac{1}{4}\left[\frac{\nu-\delta}{x}-x\right]^2\right]\ln\left|\frac{\nu-\delta-x^2-2x}{\nu-\delta+x^2-2x}\right|\\&+\frac{1}{2}\left[1-\frac{1}{4}\left[\frac{\nu+\delta}{x}+x\right]^2\right]\ln\left|\frac{\nu+\delta+x^2+2x}{\nu+\delta-x^2+2x}\right|\Bigg\},\end{aligned} \tag{A2}$$

and for $x\geq 2$:

$$\begin{aligned}\mathrm{Re}U(q^0,q,\Delta,\rho)=-\frac{2Mk_F}{\pi^2}\frac{1}{2x}\Bigg\{&x+\frac{\delta}{x}+\frac{1}{2}\left[1-\frac{1}{4}\left[\frac{\nu-\delta}{x}-x\right]^2\right]\ln\left|\frac{\nu-\delta-x^2-2x}{\nu-\delta-x^2+2x}\right|\\&+\frac{1}{2}\left[1-\frac{1}{4}\left[\frac{\nu+\delta}{x}+x\right]^2\right]\ln\left|\frac{\nu+\delta+x^2+2x}{\nu+\delta+x^2-2x}\right|\Bigg\},\end{aligned} \tag{A3}$$

where

$$\nu=\frac{2Mq^0}{k_F^2},\quad x=\frac{q}{k_F},\quad \delta=\frac{2M\Delta}{k_F^2},\quad \rho=\frac{2}{3\pi^2}k_F^3. \tag{A4}$$

In the case $q^0=0$, which we have here, the imaginary part is zero. In any case, since ImU comes either from the direct or the crossed term we can use the same expression as in Fetter and Walecka [21] (multiplying by a factor of 2) and we have

$$\mathrm{Im}U(q^0,q,\Delta,\rho)=\begin{cases}\mathrm{Im}\tilde{U}(q^0-\Delta,q,\rho) & \text{for } q^0>\Delta\ ,\\ 0 \quad \text{for } \Delta>q^0>0\ ,\\ \mathrm{Im}U(-q^0,q,\Delta,\rho) & \text{for } q^0<0\ ,\end{cases} \tag{A5}$$

where $\tilde{U}(q^0,q,\rho)$ can be expressed in a compact form as [24]

$$\mathrm{Re}\tilde{U}(q^0,q,\rho)=\frac{3}{2}\rho\frac{M}{qk_F}\left[z+\frac{1}{2}(1-z^2)\ln\left|\frac{z+1}{z-1}\right|+z'+\frac{1}{2}(1-z'^2)\ln\left|\frac{z'+1}{z'-1}\right|\right], \tag{A6}$$

$$\mathrm{Im}\tilde{U}(q^0,q,\rho)=-\frac{3}{4}\pi\rho\frac{M}{qk_F}[(1-z^2)\Theta(1-|z|)-(1-z'^2)\Theta(1-|z'|)]\frac{q^0}{|q^0|}\ , \tag{A7}$$

where Θ is the Heaviside step function and

$$z=\frac{M}{qk_F}\left[q^0-\frac{q^2}{2M}\right],\quad z'=\frac{M}{qk_F}\left[-q^0-\frac{q^2}{2M}\right]. \tag{A8}$$

For the particular case where $q^0=0$ we have for $q^0=0$, $x\le 2$,

$$\mathrm{Re}U(q^0=0,q,\Delta,\rho)=-\frac{2Mk_F}{\pi^2}\frac{1}{2x}\left\{x+\frac{1}{2}\delta-\delta\ln\left|\frac{\delta-x^2+2x}{\delta}\right|+\left[1-\frac{1}{4}\left[\frac{\delta}{x}+x\right]^2\right]\ln\left|\frac{\delta+x^2+2x}{\delta-x^2+2x}\right|\right\};$$

for $q^0=0$, $x\ge 2$,

$$\mathrm{Re}U(q^0=0,q,\Delta,\rho)=-\frac{2Mk_F}{\pi^2}\frac{1}{2x}\left\{x+\frac{\delta}{x}+\left[1-\frac{1}{4}\left[\frac{\delta}{x}+x\right]^2\right]\ln\left|\frac{\delta+x^2+2x}{\delta+x^2-2x}\right|\right\};$$

$\mathrm{Im}U(q^0=0,q,\Delta,\rho)=0$ for $q^0=0$. An interesting limiting case is when $x\ll 1$ and $x/\delta\ll 1$ in which case

$$U(q^0=0,q,\Delta,\rho)\simeq-\frac{2Mk_F}{\pi^2}\left[\frac{x}{\delta}-\frac{4}{3}\left[\frac{x}{\delta}\right]^2\right].$$

[1] D. Marlow *et al.*, Phys. Rev. C **30**, 1662 (1984).
[2] S. H. Rokni *et al.*, Phys. Lett. B **202**, 35 (1988).
[3] A. L. Williams *et al.*, Phys. Lett. B **216**, 11 (1989).
[4] M. Mizoguchi and H. Toki, Nucl. Phys. **A513**, 685 (1990).
[5] E. Oset and D. Strottman, Phys. Rev. C **44**, 468 (1991).
[6] M. Arima, K. Masutani, and R. Seki, in *Proceedings of the International Workshop on Pions in Nuclei,* Peñiscola, Spain, 1991, edited by E. Oset, M. J. Vicente-Vacas, and C. Garcia-Recio (World Scientific, Singapore), p. 292.
[7] D. J. Ernst, in [6], p. 269; D. J. Ernst and G. E. Parnell, in [3].
[8] V. Franco and H. G. Schlaile, Phys. Rev. C **41**, 1075 (1990).
[9] G. E. Parnell and D. J. Ernst, Phys. Lett. B **205**, 135 (1988).
[10] E. Oset and D. Strottman, Phys. Rev. C **42**, 2454 (1990).
[11] L. C. Liu and V. Franco, Phys. Rev. C **11**, 760 (1975).
[12] E. Oset and D. Strottman, Phys. Rev. Lett. **70**, 146 (1993); also, in [6], p. 281.
[13] D. J. Ernst (private communication).
[14] R. A. Arndt, computer code SAID, Phys. Rev. D **28**, 97 (1983).
[15] R. R. Whitehead, A. Watt, B. J. Cole, and I. Morrison, in *Advances in Nuclear Physics,* Vol. 9, edited by M. Baranger and E. Vogt (Plenum, New York, 1978).
[16] T. T. S. Kuo (private communication).
[17] S. Cohen and D. Kurath, Nucl. Phys. **73**, 1 (1965).
[18] E. Oset, D. Strottman, and G. E. Brown, Phys. Lett. **73B**, 393 (1978).
[19] A. B. Migdal, *Theory of Finite Fermi Systems and Applications to Atomic Nuclei* (Interscience, New York, 1967).
[20] J. Speth, E. Werner, and W. Wild, Phys. Rep. C **33**, 127 (1977).
[21] A. L. Fetter and J. D. Walecka, *Quantum Theory of Many Particle Systems* (McGraw Hill, New York, 1971).
[22] H. de Vries, C. W. de Jager, and C. de Vries, At. Data Nucl. Data Tables **36**, 495 (1987).
[23] G. R. Burleson (private communication).
[24] E. Oset, P. Fernández de Córdoba, L. L. Salcedo, and R. Brockmann, Phys. Rep. **188**, 79 (1990).